

# Producing Airborne Ultrasonic 3D Tactile Image by Time Reversal Field Rendering

Seki Inoue<sup>1†</sup>, Yasutoshi Makino<sup>2</sup> and Hiroyuki Shinoda<sup>2</sup>

<sup>1</sup>Graduate School of Information Science and Technology, The University of Tokyo, Tokyo, Japan  
(Tel: +81-3-5841-6368; E-mail: seki\_inoue@ipc.i.u-tokyo.ac.jp)

<sup>2</sup>Department of Complexity Science and Engineering, The University of Tokyo, Tokyo, Japan  
(Tel: +81-3-5841-6926; E-mail: {yasutoshi\_makino, hiroyuki\_shinoda}@k.u-tokyo.ac.jp)

**Abstract:** In this paper, we propose a method to render ultrasound pressure distribution in an inhomogeneous field by surrounding phased array especially for the purpose of invoking tactile sensation to human skins. Our previous work showed that ultrasound stationary radiation force can invoke tactile sensation for user's finger in 3D cavity which is surrounded by ultrasound transducers. However, disturbance of an acoustic wave field by user's hand is not negligible and therefore the sensed haptic force decreases. In addition, ways to present arbitrary spatial form are also desired. The proposed method renders the pressure field and reconstructs it by finite element method and time reversal method. This method can be applied to inhomogeneous field with the presence of fingers or palms and can create complicated images.

**Keywords:** Haptic Interface, Airborne Ultrasound Tactile Display, 3D Tactile Image, Time Reversal Method

## 1. INTRODUCTION

Tactile sensations for aerial floating 3D images are greatly desired for years. It is expected that haptic information over 3D images improve the usability of interactive applications. To realize this, the methods to invoke tactile sensation to the user have some requirements. First, the haptic device should not affect optical pictures. Second, the haptic device should not hinder user's actions. Third, the position or shape of presented haptic objects should be flexible.

Many mechanical approaches have been proposed for 3D haptic presentation. For example, using pen-type pointing devices like PHANTOM™ or glove-type master-slave systems[1] can present strong and accurate force feedback. However, in this strategy, skin and the device are always in contact and leading to prevent free motion. Recent vibrotactile approaches have made the devices simplified and wearable, however users still have to touch the virtual objects via special devices[2]. Other approaches to present tactile sensation at a distance without any direct contact have been also proposed. For example, using air-jets enables to realize non-contact force[3][4][5], however its spatial and temporal profiles are quite rough.

The airborne ultrasound tactile method has been investigated. This method utilizes airborne ultrasound and its radiation force to skin. Using ultrasound phased array, focused ultrasound is emitted and cause radiation pressure sensed as tactile sensation. In [6], we proposed a method using stationary wave and create a single virtual sphere. This virtual aerial sphere is sensed with compliant feedback and omni-directionary pinchable. The focus created by stationary wave is smaller than that of traveling wave and therefore the density of energy become higher. However, it is pointed out that the stationary wave field is interfered by user's finger and the pressure level decreases.

Furthermore, ways to present arbitrary spatial form are also expected.

In [7], Hasegawa et. al. proposed a calculation method for arbitrary three-dimensionally distributed amplitude with transducers located in three-dimensional arrangement. This method introduce a simple distance-based propagation model and inversely solve it by applying least squares method to resulting sound pressure distribution. This method, however, have difficulty in applying for inhomogeneous field that is disturbed by user's hand.

In this paper, we propose a method to cope with the interference of fingers and present multi spheres simultaneously by using time reversal method. The time reversal method is known well in the field of sensing such as ultrasound scanners or medical therapy. On this proposed method, the FEM calculation is executed under the assumption that fingers and monopole ultrasound source(s) exist and the time reversal wave is acquired and emitted from the phased array. We demonstrated numerical and measurement experiments and as a result we got more powerful sensation for double spheres.

## 2. PRINCIPLE

### 2.1. Airborne Ultrasound Tactile Display

The airborne ultrasound tactile display has been proposed which can cause tactile sensation to human skins remotely and with no worn devices[8][9]. Using phased array, a focal point is steered at any point in the workspace. In the conventional way, proper amplitude and phase of transducer at  $r$  which creates a single radiation pressure focus in homogeneous field at  $r_f$  is given as[6]:

$$p(r, t) = A \sin \left( 2\pi f(t + \frac{|r - r_f|}{c}) \right) \quad (1)$$

This distance-based method is quite simple and its small computing resources is enough to handle with FP-

† Seki Inoue is the presenter of this paper.

GAs[10]. However, this method does not work for inhomogeneous field. Especially in tactile display use, interference by fingers is not negligible.

## 2.2. Spatial Rendering for Inhomogeneous Field

Several attempts to make ultrasonic foci in inhomogeneous field have been investigated in the field of medical therapy such as hyperthermia[11][12][13]. The conventional methods called Inverse Filter (IF) or Pseudoinverse are more or less invasive and need needle hydrophones implanted in the region of interest. Another approaches called Time Reversal (TR) is useful of practical use for hyperthermia therapy or fish sonar. This approach is non-invasive but instead "beacons" i.e. dominant wave reflector at foci are required.

For tactile display, neither invasive audio source nor beacons at foci (surface of skins) can be expected. On the other hand, we can premise following two assumptions, 1) the position of user's hand can be optically measured and 2) the dominant scatter occurs only on surface of skin. In this situation, the propagation model can be constructed from the optical point cloud measurements and solved by numerical analysis.

Both Inverse Filter and Time Reversal Method can be solved by numerical analysis. However considering general numerical analysis such as FEM or BEM is highly heavy computation task, we employ TR method which has lesser computation cost.

## 2.3. Time Reversal Method

In a lossless propagation medium, the propagation equation of an acoustic pressure field is described as below[14]:

$$\nabla \cdot \left( \frac{\nabla p}{\rho} \right) - \frac{1}{\rho c^2} \frac{\partial^2 p}{\partial t^2} = 0. \quad (2)$$

where  $p$  is acoustic pressure,  $\rho$  is density of the medium and  $c$  is velocity of waves. Since this equation contains only even order time derivative terms, the time reversal wave is appeared as another solution, i.e. if  $p(r, t)$  is a solution of this equation, then  $p(r, -t)$  is also a solution. These waves propagate opposite direction each other.

When  $p_f(r, t | r_0)$  represents an acoustic field which has a focal point at a point  $r_0$ . Then, the time reversal field  $p_{mp}(r, t | r_0) = p_f(r, -t | r_0)$  is equivalent to the field that has single monopole at  $r_0$ . This fact suggests that if we have  $p_{mp}(r_{t_i}, t | r_0)$  at transducers at  $r_{t_i}$  respectively, a focal point at  $r_0$  can be reconstructed by emitting the time reversal wave from transducers.

Now let us assume that piezo transducers emit single frequency and the acoustic field is reciprocal and linear time invariant, the impulse response from  $r_0$  to  $r_{t_i}$  is described as below:

$$h(r_0 | r_{t_i}, t) = h(r_{t_i} | r_0, t) \quad (3)$$

$$= a_{r_0, r_{t_i}} \delta(\phi_{r_0, r_{t_i}} / \omega - t) \quad (4)$$

where  $h(r_0 | r_{t_i}, t)$  is the impulse response from  $r_0$  to  $r_{t_i}$ ,  $a$  is attenuation factor and  $\phi$  indicates the phase delay.

According to Huygens-Fresnel principle, acoustic pressure at transducer  $s(r_{t_i}, t)$  for desired distribution  $q(r, t)$  is described as below:

$$s(r_{t_i}, t) = \int_V q(r_0, t) \otimes_t h(r_0 | r_{t_i}, t) dr_0 \quad (5)$$

Then, we can reconstruct the distribution by emitting  $s(r_{t_i}, -t)$  from transducers at  $r_{t_i}$ . The reconstructed distribution is obtained as:

$$\begin{aligned} p(r, t) &= \int_V \int_{\partial V} q(r_0, -t) \\ &\quad \otimes_t a_{r_0, r_{t_i}} \delta(\phi_{r_0, r_{t_i}} / \omega - t) \\ &\quad \otimes_t a_{r, r_{t_i}} \delta(\phi_{r, r_{t_i}} / \omega + t) dr_0 dr_{t_i} \quad (6) \\ &= \int_V \int_{\partial V} a_{r_0, r_{t_i}} a_{r, r_{t_i}} q(r_0, -t) \\ &\quad \otimes_t \delta\left(\frac{\phi_{r_0, r_{t_i}} - \phi_{r, r_{t_i}}}{\omega} - t\right) dr_0 dr_{t_i} \quad (7) \end{aligned}$$

So, the wave is refocused at the point where  $\phi_{r_0, r_{t_i}} - \phi_{r, r_{t_i}} = \text{const.}$  holds for any  $r_{t_i}$ . Except for mal-arrangements of transducers, foci appear at  $r = r_0$ .

The reconstructed field is not the exactly same as designed field when many foci are placed. The inverse filter method has higher degree of freedom rather than TR method. However, in terms of the efficiency of computation cost, the time reversal method is much superior.

### 2.3.1. FEM Based Time Reversal Method

The ordinary time reversal method needs wave reflection source such as kidney stones in tissue or fishes in water. Focal points are emerged by the time reversal of such reflected wave. In proposed situation, however, the reflection sources are not presented, so we use FEM computation to obtain the wave to traverse.

Now let us assume that desired sound field is time-harmonic stationary wave i.e.  $q(r, t) = q(r)e^{-j(\omega t + \theta)}$ . Then this system is also time-harmonic, and therefore the governing equation is described by extending eq.(2).

$$\nabla \cdot \left( \frac{\nabla p}{\rho} \right) + \frac{\omega^2}{\rho c^2} p = -q \quad (8)$$

where  $\rho$  is density of the medium and  $c$  is sound speed.  $p$  is represented like below:

$$p = A e^{-j\phi} \quad (9)$$

and the time reversal is:

$$p = A e^{j\phi} \quad (10)$$

So, we can use so called stationary FEM solvers and obtain time reversal signal by sign inversion of phase term.

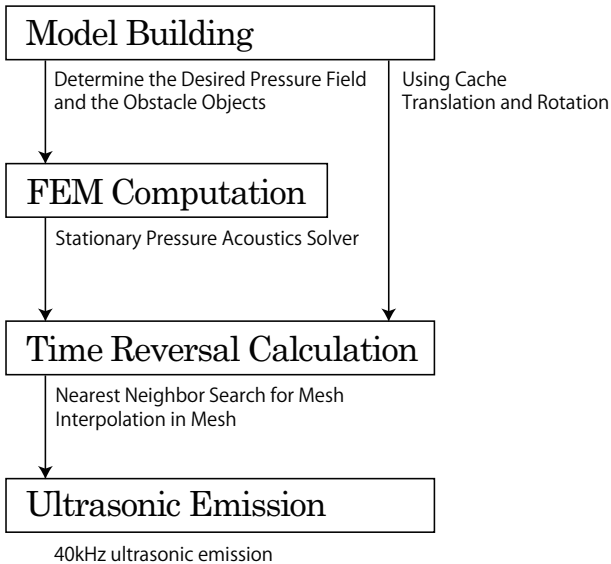


Fig. 1 The outline of proposed system.

### 3. IMPLEMENTATION

The proposed system consists by four modules. Firstly, desired acoustic pressure distribution and obstacle object models in field is built. This means that focal points and the location of fingers and palm is modeled for next FEM step. Secondly, FEM is computed. Thirdly, time reversal signals at each transducers are calculated. Finally, transducers emit ultrasonic acoustic wave. The outline of this proposed system is shown in Fig. 1.

#### 3.1. Model Building

For FEM computation, the location of focal points and objects which interferes the wave propagation should be determined. The main obstacle object is finger in this situation. The user's finger and focal point come in contact with each other when user touches the aerial haptic image. It is desirable that the location of hands is observed in real time for interactive applications. An optical based measurement is conceivable but in this paper we use pre-arranged models for preliminary investigation.

As stated in [6], the phased array around the field behaves as perfectly matched boundary because the impedance of transducers used in phased array should be designed to match for the medium i.e. air. Therefore, we don't have to take the existence of phased arrays into account in this phase.

#### 3.2. FEM Computation

The finite element method is well-known and widely used approach to solve partial differential equations. The governing equation to be solved is eq. (8) as led above. It is known that the accuracy of FEM is largely affected by the size of mesh. It is empirically pointed out that the mesh size should be  $\lambda/6 \sim \lambda/10$  where  $\lambda$  is wave length[15]. We use COMSOL Multiphysics for experiment described below.

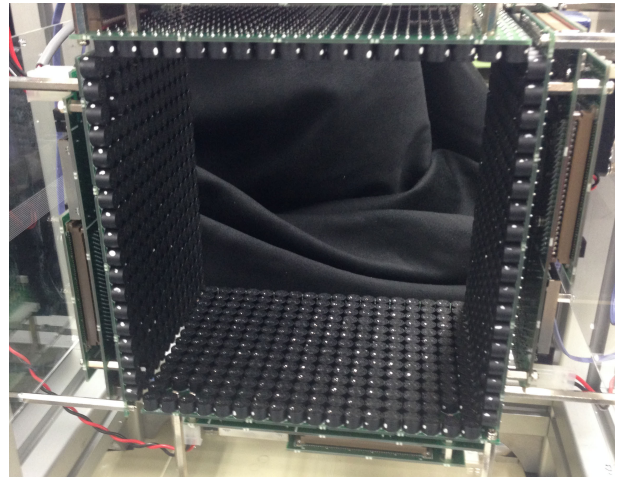


Fig. 2 An overall picture of the phased array. 4 arrays with 249 transducers, a total of 996 transducers were arranged that forms rectangular parallelepiped.

#### 3.3. Time Reversal Calculation

To calculate time reversal signal for each transducers, the result of FEM computation at the location of transducers i.e.  $s(r_{t_i}, t)$  is needed. Since the locations of transducers do not affect the FEM result as discussed at section 3.1, the single FEM result can be applied for translated or rotated geometry. This means that we can extract  $s(r_{t_i}, t)$  for any isomorphic models in terms of translation and rotation.

Furthermore, interpolations are needed because the data structure is discrete. We use 4-nearest neighbor search and tetrahedron-interpolation. The implementation was done by FLANN library[16].

#### 3.4. Ultrasonic Emission

We implemented the phased array as shown in figure 2. In this phased array, transducers were arranged to surround rectangular parallelepiped field. One side of rectangular parallelepiped mounts 249 transducers in 14 cm  $\times$  18 cm area. Totally 996 transducers are arranged around 14 cm  $\times$  14 cm  $\times$  18 cm volume.

The drive frequency was 40kHz and the amplitude and the phase of each transducers were dynamically controllable in 256-level quantization respectively via USB 2.0 interface.

### 4. EXPERIMENT

We performed numerical and measurement experiments with the implementation described above. We prepared a model that mocks a thumb and a forefinger as an obstacle model shown in Fig. 3. This model was placed at the centre of the field and the property for FEM computing was set as Table 4. The entire field model prepared for FEM computing was shown in Fig. 4. The dual monopole sound sources were placed at the top inner sides of pseudo-fingers.

Using this field model, the FEM computing were done and the result is figured as Fig. 5. The consumed compu-

Table 1 Property of objects for FEM computing. Under the assumption that the obstacle object is finger, the properties are applied as that of water.

|                       | Air   | Obstacle Model |
|-----------------------|-------|----------------|
| $c[\text{m/s}]$       | 343.1 | 1481           |
| $\rho[\text{kg/m}^3]$ | 1.293 | 999.7          |

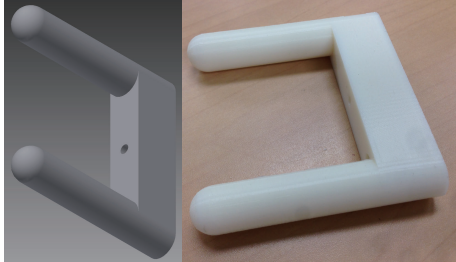


Fig. 3 The overview of an obstacle model. This mocks up thumb and forefinger.

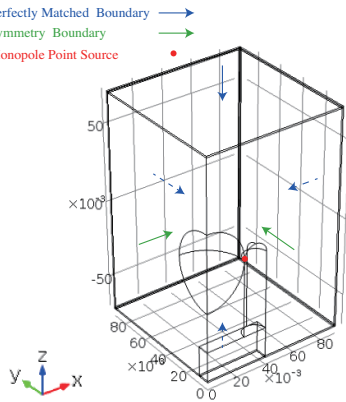


Fig. 4 The field model prepared for FEM computing.

The front two planes are symmetrical planes and the back two planes are perfectly matched layer. The monopole sound source point is set at a point of contact between obstacle object and centre sphere. With the symmetrical plane, there are two sound sources in whole model.

tation time is about 120 minutes. Although we used very fine meshes and a strict permissible error for preliminary experiment, we recognize this consumption time is very important problem to be solved.

#### 4.1. Numerical Experiment

To visualize the acoustic field of the working field, numerical simulation of the ultrasound emission by FEM was conducted. The transducers were treated as monopole sound sources and placed at the same geometry as that of hardware implementation. Fig. 6 indicates the normalized acoustic pressure distribution for proposed method. The focal points successfully appeared at the side of finger object. Note that there are two foci in whole field with the symmetrical plane.

For comparison, another experiment when ignoring an obstacle was also done. To be exact, the emission of the transducers were determined only by distance i.e. under

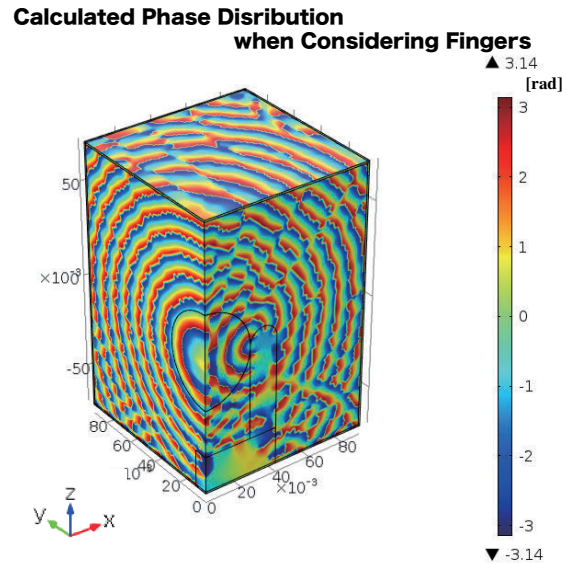


Fig. 5 The phase distribution of the FEM computation result.

#### Normalized Simulated Acoustic Pressure Distribution when Considering Fingers

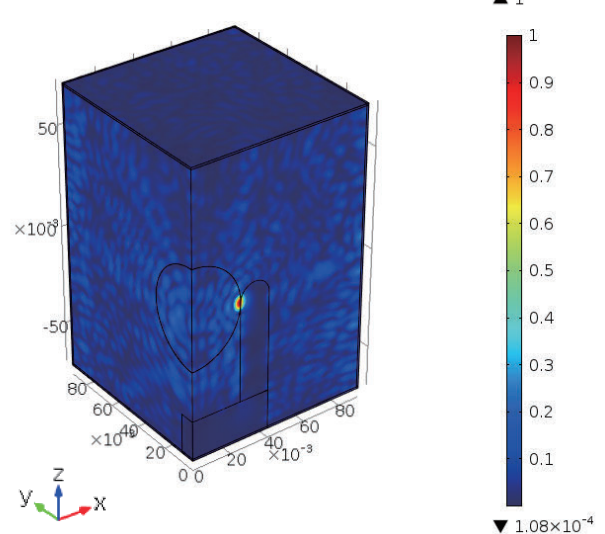


Fig. 6 The simulated normalized acoustic pressure distribution for proposed method. The focal points successfully appeared at the side of the finger.

the assumption described below:

$$h(r_{t_i}|r_0, t) = \delta\left(\frac{|r_0 - r_{t_i}|}{c} - t\right) \quad (11)$$

The result of the control experiment is shown in Fig. 7. The focal points appeared at the side of finger object but the intensity remains only about half of proposed method.

#### 4.2. Measurement Experiment

To confirm the result of numerical simulation, the actual acoustic pressure distribution was measured. As shown in Fig. 8, the microphone with diameter of 1/4 inch was pointed in parallel with the phased arrays. Using

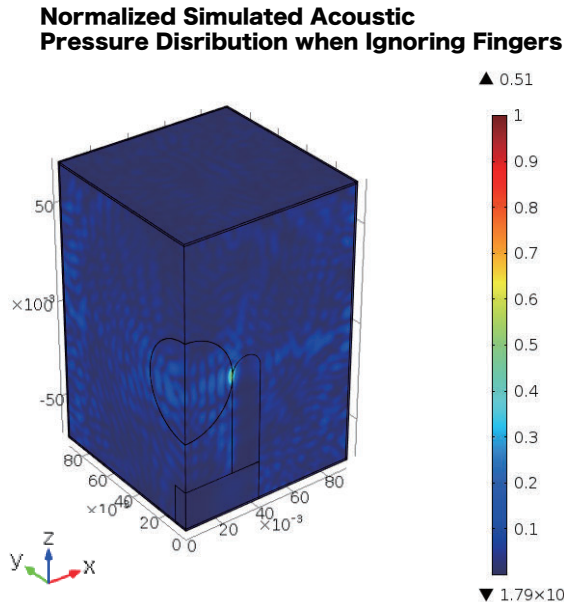


Fig. 7 The simulated normalized acoustic pressure distribution for control experiment. The normalization is consisted with Fig. 6. The focal point appeared at the side of the finger but the intensity was only half of proposed method.

motorized 3-axis stage, the acoustic pressure was measured around a focal point by 0.25 mm intervals.

The experiments were done for two cases. First one was the case which consider the presence of fingers corresponding to Fig. 6 in numerical experiments. Second was the case which ignores the presence of fingers corresponding to Fig. 7.

The results are indicated on Fig. 9 and Fig. 10 respectively. Although there are two foci in the workspace, we show one of them on these figures. On Fig. 9, the focal point appeared near field region of pseudo-finger model as designed. And on Fig. 10, the focal point was still appears but the peak intensity was 0.60 as low as of considering finger's affection. Note that the ratio of the intensity of the peaks among two condition was very similar to that of numerical experiments.

## 5. CONCLUSION

In this paper we proposed a method to design the ultrasound acoustic pressure distribution with 3D arranged phased array. This method uses time reversal method and computed with FEM. It is proposed for the purpose to apply for airborne ultrasound tactile display and can be useful for inhomogeneous field. Numerical and measurement experiments are conducted and it is discovered that the proposed method can create multiple focal points while cope with the interference of artificial fingers.

As further works, there are some problems that should be solve.

Firstly, the FEM computation costs a lot of computing resources and take long operation time. It is desirable that the rendering is done real-timely when this method

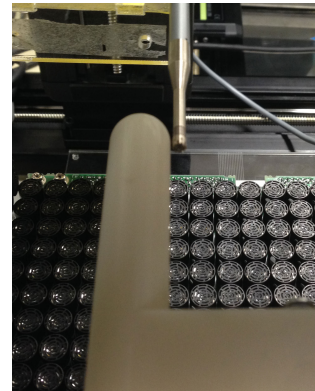


Fig. 8 The scene of experiments to measure the actual pressure distribution. The microphone whose diameter was 1/4 inch were mounted on 3-axis motorized stage and was pointed in parallel with phased array and pseudo-finger model.

## Normalized Measured Acoustic Pressure Distribution when Considering Fingers

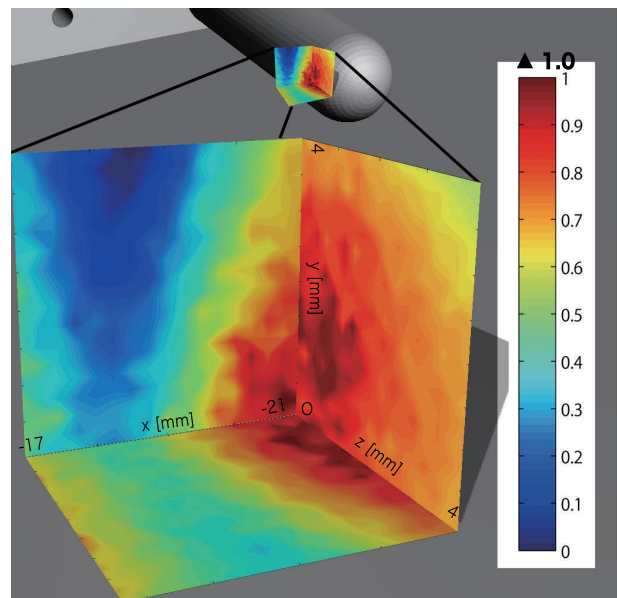


Fig. 9 The normalized acoustic pressure distribution of measurement experiment with considering the presence of fingers (interpolated). Using motorized 3-axis stage, the acoustic pressure was measured around a focal point by 0.25 mm intervals. The focal point appeared near field region of pseudo-finger model as designed. The values were normalized with the maximum value observed among Fig.9 and Fig.10.

is applied to interactive applications. The mesh size has great influence on the amount of computing cost but the larger mesh size may cause deterioration of the simulation error. It is expected to investigate and optimize the mesh size, models and FEM solver.

Secondly, the model building for FEM should be adaptive. It means that the model should reflects the actual location of obstacle objects by sensing. The optical point group sensors may be useful. Furthermore, since trans-

### Normalized Measured Acousitc Pressure Distribution when Ignoring Fingers

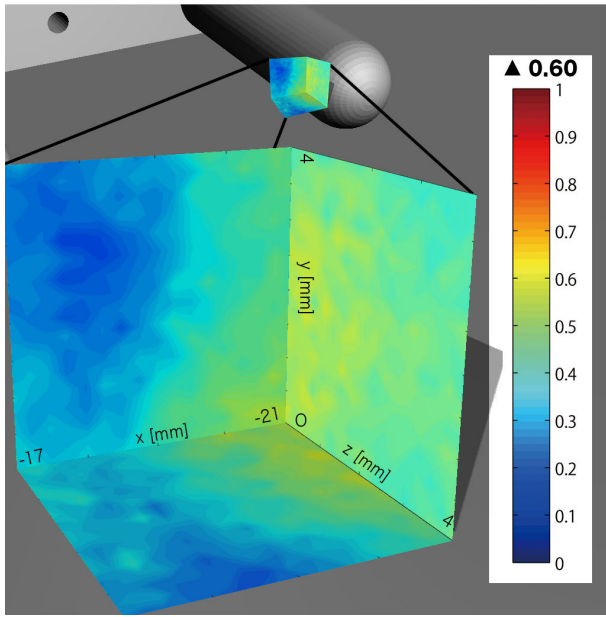


Fig. 10 The normalized acoustic pressure distribution of measurement experiment with considering the presence of fingers (interpolated). Using motorized 3-axis stage, the acoustic pressure was measured around a focal point by 0.25 mm intervals. The focal point appears near field region of pseudo-finger model but the intensity is about 0.6 times as low as of proposed method. The values were normalized with the maximum value observed among Fig.9 and Fig.10.

ducers can use as sensor, it may be possible to create arbitrary field with self-adaptive by sensing and emitting ultrasound simultaneously.

## REFERENCES

- [1] D. Jack, R. Boian, A.S. Merians, M. Tremaine, G.C. Burdea, S.V. Adamovich, M. Recce, and H. Poizner: Virtual reality-enhanced stroke rehabilitation, *Neural Systems and Rehabilitation Engineering, IEEE Transactions on*, Vol. 9, No. 3, pp. 308–318, 2001.
- [2] K. Minamizawa, Y. Kakehi, M. Nakatani, S. Mi-hara, and S. Tachi: Techtile toolkit: a prototyping tool for designing haptic media, *ACM SIGGRAPH 2012 Emerging Technologies*, pp. 22:1–22:1, SIGGRAPH ’12, ACM, 2012.
- [3] Y. Suzuki and M. Kobayashi: Air jet driven force feedback in virtual reality, *Computer Graphics and Applications, IEEE*, Vol. 25, No. 1, pp. 44–47, 2005.
- [4] S. Gupta, D. Morris, S.N. Patel, and D. Tan: Air-wave: Non-contact haptic feedback using air vortex rings, *Proceedings of the 2013 ACM International Joint Conference on Pervasive and Ubiquitous Computing*, pp. 419–428, UbiComp ’13, ACM, 2013.
- [5] R. Sodhi, I. Poupyrev, M. Glisson, and A. Israr: Aireal: Interactive tactile experiences in free air, *ACM Trans. Graph.*, Vol. 32, No. 4, pp. 134:1–134:10, 2013.
- [6] S. Inoue and H. Shinoda: A pinchable aerial virtual sphere by acoustic ultrasound stationary wave, *Haptics Symposium (HAPTICS), 2014 IEEE*, pp. 89–92, 2014.
- [7] K. Hasegawa and H. Shinoda: A method for distribution control of aerial ultrasound radiation pressure for remote vibrotactile display, *SICE Annual Conference (SICE), 2013 Proceedings of*, pp. 223–228, 2013.
- [8] T. Hoshi, M. Takahashi, T. Iwamoto, and H. Shinoda: Noncontact tactile display based on radiation pressure of airborne ultrasound, *Haptics, IEEE Transactions on*, Vol. 3, No. 3, pp. 155–165, 2010.
- [9] T. Carter, S.A. Seah, B. Long, B. Drinkwater, and S. Subramanian: Ultrahaptics: Multi-point mid-air haptic feedback for touch surfaces, *Proceedings of the 26th Annual ACM Symposium on User Interface Software and Technology*, pp. 505–514, UIST ’13, ACM, 2013.
- [10] K. Hasegawa and H. Shinoda: Aerial display of vibrotactile sensation with high spatial-temporal resolution using large-aperture airborne ultrasound phased array., *World Haptics*, pp. 31–36, 2013.
- [11] M.T. Buchanan and K. Hyynen: Design and experimental evaluation of an intracavitary ultrasound phased array system for hyperthermia, *Biomedical Engineering, IEEE Transactions on*, Vol. 41, No. 12, pp. 1178–1187, 1994.
- [12] P. VanBaren, R. Seip, and E.S. Ebbini: Real-time dynamic focusing through tissue inhomogeneities during hyperthermia treatments with phased arrays, *Ultrasonics Symposium, 1994. Proceedings., 1994 IEEE*, Vol. 3, pp. 1815–1819vol.3, 1994.
- [13] F. Vignon, J. deRosny, J.-F. Aubry, and M. Fink: Optimal adaptive focusing through heterogeneous media with the minimally invasive inverse filter, *The Journal of the Acoustical Society of America*, Vol. 122, No. 5, , 2007.
- [14] M. Fink: Time reversal of ultrasonic fields. i. basic principles, *Ultrasonics, Ferroelectrics and Frequency Control, IEEE Transactions on*, Vol. 39, No. 5, pp. 555–566, 1992.
- [15] M. Steffen and N. Bodo: Computational Acoustics of Noise Propagation in Fluids - Finite and Boundary Element Methods, Springer, 2008.
- [16] M. Muja and D.G. Lowe: Fast approximate nearest neighbors with automatic algorithm configuration, *International Conference on Computer Vision Theory and Application VISSAPP’09*, pp. 331–340, INSTICC Press, 2009.